UNBIASED FIR ESTIMATES VS. THE SAWTOOTH-CORRECTED GPS-BASED MEASUREMENTS : EXPERIMENTAL EVALUATION

Y. S. Shmaliy, L. Arceo-Miquel, J. Munoz-Diaz, and O. Ibarra-Manzano
Guanajuato University, FIMEE, Mexico
E-mail: *shmaliy@salamanca.ugto.mx*

Abstract

We show that, owing to small noise and smoothed excursions, the unbiased FIR filtering algorithm produces more accurate estimates of the TIE model of a local clock than the sawtooth-less GPS-based measurements. The algorithm becomes much more efficient in estimating the fractional frequency offset and higher order states. For the algorithm to work with minimum errors, the optimal time step τ_{opt} and number of the points in the average N_{opt} must be ascertained in the sense of the minimum mean-square error (MSE) for each of the clock states. The relevant dependencies of N_{opt} on τ_{opt} are found experimentally for a crystal clock. The trade-off between the estimates and sawtooth-less measurements is illustrated graphically.

INTRODUCTION

Evaluation of the time interval error (TIE) of a local clock is easily provided using the commercially available GPS timing receivers. The problem is that the GPS-based measurements with, for example, the Motorola family of the receivers such as the SynPaQ III GPS Sensor, induce the sawtooth noise of about ±50 ns owing to the principle of the one pulse per second (1PPS) signal formation utilized in the receiver.[1] By means of the receiver **[1]** or auxiliary software **[2]**, the sawtooth noise may be reduced by a factor of about 10. In the measurements of the TIE, it can also be suppressed using the recently designed unbiased finite impulse response (FIR) filter and algorithm **[3,4]** allowing for an error less than that obtained by a standard Kalman filter. The first comparative results in estimating the TIE have shown **[5,6]** that the FIR estimates become much more efficient than the sawtooth correction if the unbiased FIR filter is optimized for the time step τ_{opt} (obtained by thinning in time the 1PPS pulses) and the number of the points N_{opt} in the average.

In this paper, we take a more precise look at the problem comparing the TIE estimates of a local crystal clock to provided simultaneously the GPS-based sawtooth-less measurements and measurements for a reference rubidium clock. We also present the results of the experimental evaluation of the optimal N_{opt} and τ_{opt} for several states of the local clock, thereby answering the question: what are optimum values τ_{opt} and N_{opt} for the unbiased FIR filtering algorithm in the sense of the minimum mean-square error (MSE) in each of the estimates?

[1]Clark and Hambly reported in **[1]** that, in the modified receivers, the noise bounds are reduced to ±13 ns.

AN UNBIASED FIR FILTERING ALGORITHM

Before discussing the results of the experimental studies, it is in order first to describe in brief the TIE model of a local clock and the unbiased FIR filtering algorithm proposed in **[4]** and thereafter studied in **[6]**.

TIE MODEL OF A CLOCK

Most commonly, the TIE polynomial model of a clock projects ahead on a horizon of N points from the starting point n = 0 with the Kth-degree Taylor polynomial:

$$x_1(n) = \sum_{p=0}^{K} x_{p+1} \frac{\tau^p n^p}{p!} + w_1(n,\tau)$$

$$= x_1 + x_2 \tau\, n + \frac{x_3}{2}\tau^2 n^2 + \frac{x_4}{6}\tau^3 n^3 \ldots + w_1(n,\tau), \tag{1}$$

where $x_{l+1} \equiv x_{l+1}(0)$, $l \in [0, K]$, are initial states of the clock and $w_1(n,\tau)$ is a clock noise with known properties. By extending the time derivatives of the TIE model to the Taylor series, the signal and observation equations become, respectively,

$$\lambda(n) = \mathbf{A}(n)\,\lambda(0) + \mathbf{w}(n,\tau), \tag{2}$$

$$\xi(n) = \mathbf{C}\,\lambda(n) + \mathbf{v}(n), \tag{3}$$

where

$$\lambda(n) = [x_1(n)\; x_2(n)\; \ldots\; x_{K+1}(n)]^T$$

is a $(K + 1) \times 1$ vector of the clock states and

$$\mathbf{A}(n) = \begin{bmatrix} 1 & \tau n & \tau^2 n^2/2 & \cdots & (\tau n)^K/K! \\ 0 & 1 & \tau n & \cdots & (\tau n)^{K-1}/(K-1)! \\ 0 & 0 & 1 & \cdots & (\tau n)^{K-2}/(K-2)! \\ \vdots & \vdots & \vdots & \ddots & \vdots \\ 0 & 0 & 0 & \cdots & 1 \end{bmatrix}. \tag{4}$$

is a $(K + 1) \times (K + 1)$ time-varying system matrix.

For an equal number of the states and measurements, the observation vector is described by

$$\xi(n) = [\xi_1(n)\; \xi_2(n) \ldots \xi_{K-1}(n,\tau)]^T$$

and the $(K + 1) \times (K + 1)$ measurement matrix **C** is typically unit. The $(K + 1) \times 1$ clock noise vector is described by

$$\mathbf{w}(n,\tau) = [w_1(n,\tau)\ w_2(n,\tau) \ldots w_{K+1}(n,\tau)]^T$$

with the components caused by the oscillator noises. Finally, the noise vector

$$\mathbf{v}(n) = [v_1(n)\ v_2(n) \ldots v_{K-1}(n)]^T$$

contains correlated or uncorrelated components that are not obligatory white Gaussian. The GPS noise **v** (n) dominates on a horizon N; that is, typically, $\langle w_u^2(n,\tau)\rangle_N << \langle v_l^2(n)\rangle_N$. Therefore, **w** ($n$, τ) is neglected in (3) and in the FIR procedure **[4]**.

AN UNBIASED FIR FILTERING ALGORITHM

The unbiased FIR filtering algorithm shown in Fig. 1 and Fig. 2 gives a typical structure of the sawtooth noise induced by the receiver and provided at one of its outputs as the negative sawtooth. It may be seen that the noise is mean-zero with the upper and lower bounds of ±50 ns and uniformly distributed. The clock first state estimate $\hat{x}_1(n)$ (TIE) is obtained with $h_K(i)$ at a horizon of N_K points. The observation $\xi_2(n)$ for the second state $x_2(n)$ (fractional frequency offset) is then formed by increments of $\hat{x}_1(n)$. Accordingly, $\hat{x}_2(n)$ is achieved with $h_{K-1}(i)$ at a horizon of N_{K-1} points. Inherently, the first accurate value of $\hat{x}_2(n)$ appears at the $(N_K + N_{K-1})$th point starting from $n = 0$. Finally, the last state estimate $\hat{x}_{K+1}(n)$ is calculated with $h_0(i)$ at a horizon of N_0 points, using $\xi_{K+1}(n)$ that is formed in the same manner as $\xi_2(n)$. The first correct value of $\hat{x}_{K+1}(n)$ appears thus at the $(N_K + N_{K-1} + \ldots + N_0)$th point.

The unique low order FIRs for the algorithm (Fig. 1) are derived in **[4]** and given below.[2]

$$h_0(i) = \frac{1}{N}, \tag{5}$$

$$h_1(i) = \frac{2\,(2N-1) - 6\,i}{N\,(N+1)}, \tag{6}$$

$$h_2(i) = \frac{3\,(3N^2 - 3N + 2)\ - 18\,(2N-1)\,i\ + 30\,i^2}{N\,(N+1)\,(N+2)}, \tag{7}$$

$$h_3 = \frac{8\,(2N^3 - 3N^2 + 7N - 3) - 20\,(6N^2 - 6N + 5)\,i\ + 120\,(2N-1)\,i^2 - 140\,i^3}{N\,(N+1)\,(N+2)\,(N+3)}, \tag{8}$$

having the inherent common properties:

[2] The kernel (6) was first derived in **[3]**.

$$h(i) \;=\; \begin{cases} h(i),\ 0 \le i \le N-1 \\ 0,\ \textit{otherwise} \end{cases}, \quad \sum_{i=0}^{N-1} h(i) \;=\; 1.$$

Depending on the model degree K, we thus have several particular realizations of the algorithm. If a noiseless model is assumed to be time-invariant, $K = 0$, the only nonzero state is the TIE and the estimate of the TIE is provided by simple averaging,

$$\hat{x}_1(n) = \frac{1}{N_0} \sum_{i=0}^{N_0-1} \xi(n-i). \tag{9}$$

The linear model, $K = 1$, is processed for two states by

$$\hat{x}_1(n) = \sum_{i=0}^{N_1-1} h_1(i) \xi_1(n-i), \tag{10}$$

$$\hat{x}_2(n) = \frac{1}{\tau N_0} \sum_{j=0}^{N_0-1} [\hat{x}_1(n-j) - \hat{x}_1(n-j-1)]. \tag{11}$$

For the quadratic model, $K = 2$, the 3-state unbiased FIR batch algorithm becomes

$$\hat{x}_1(n) = \sum_{i=0}^{N_2-1} h_2(i) \, \xi_1(n-i), \tag{12}$$

$$\hat{x}_2(2) = \frac{1}{\tau} \sum_{j=0}^{N_1-1} h_1(j) [\hat{x}_1(n-j) - \hat{x}_1(n-j-1)], \tag{13}$$

$$\hat{x}_3(n) = \frac{1}{\tau N_0} \sum_{r=0}^{N_0-1} [\hat{x}_2(n-r) - \hat{x}_2(n-r-1)]. \tag{14}$$

Finally, if we assume a cubic model, $K = 3$, the algorithm is formed with

$$\hat{x}_1(n) = \sum_{i=0}^{N_3-1} h_3(i) \; \xi_1(n-i), \tag{15}$$

$$\hat{x}_2(n) = \frac{1}{\tau} \sum_{j=0}^{N_2-1} h_2(j) \, [\hat{x}_1(n-j) - \hat{x}_1(n-j-1)], \tag{16}$$

$$\hat{x}_3(n) = \frac{1}{\tau} \sum_{p=0}^{N_1-1} h_1(p) \, [\hat{x}_2(n-p) - \hat{x}_2(n-p-1)], \tag{17}$$

$$\hat{x}_4(n) = \frac{1}{\tau N_0} \sum_{r=0}^{N_0-1} [\hat{x}_3(n-r) - \hat{x}_3(n-r-1)], \tag{18}$$

As may be seen, the calculus (9)–(18) needs setting two constants, N and τ, for each of the estimates to be unbiased and near optimal in the sense of the minimum MSE.

OPTIMUM N AND τ

Experimental evaluation of N_{opt} and τ_{opt} for each of the unbiased FIR filters in (9)–(18) was provided for the crystal clock embedded in the Stanford Frequency Counter SR620 and rubidium clock attached to SR625. Measurements were made with the GPS timing sensor SynPaQ III and SR620 for $\tau = 1$ s (GPS - measurement). Simultaneously, to obtain reference trends for each of the estimates, the TIE of the local clock had been measured for the atomic clock (we exploit the rubidium oscillator attached to SR625 or cesium clock Cs III of Symmetricom). Initial time and frequency shifts between two measurements were then eliminated statistically and a transition to $\tau > 1$ s was provided by the 1PPS measurements thinning in time. The difference between each estimate and the reference trend or its time derivatives is evaluated in the sense of the MSE and the optimal values N_{opt} and τ_{opt} are found for the minimum MSEs.

In our experiment, for signal processing, we exploited measurements obtained during about one day. Therefore, the upper bound of τ was limited by 10^4 s, inducing two principal limitations for N_{opt} and τ_{opt}:

• Finite data of measurements (about 1 day) affecting the estimates if $\tau > 10^3$ s.

• Long-term phase drifts in the reference clocks affecting estimates.

Below we bring results of experimental evaluations of τ_{opt} and N_{opt} for several states of a local crystal clock via the GPS-based and rubidium-based measurements.

THE FIRST CLOCK STATE (TIE)

Fig. 2 illustrates an evaluation of N_{opt} vs. τ for the first clock state (TIE) with the four algorithms. A common conclusion is that the minimum root-mean-square error (RMSE) corresponds to $\tau = 1$ s by all of the algorithms and, hence, estimating the TIE does not require thinning in time the measured data. For TIE, τ_{opt} is exactly 1 s. One may also observe that simple averaging provides for with a minimum number $N_{0(opt)}$ of the points among all other filters. However, the RMSE in simple averaging (5) is larger than in linear and quadratic kernels, (6) and (7), respectively. The cubic kernel (8) produces even larger error than in (6) and (7). Based upon this, we identify the TIE model of the investigated clock to be either linear or quadratic on the horizon of N_{opt} points.

THE SECOND CLOCK STATE (FRACTIONAL FREQUENCY OFFSET)

To ascertain τ_{opt} and N_{opt} for the second clock state (fractional frequency offset), one first needs to estimate optimally the TIE for the optimal N and τ taken from Fig. 2. Thereafter, by the algorithm (Fig. 1), the weighted increments of these estimates serve as measurements for the second state. Fig. 3 shows the results of evaluating the N_{opt} vs. τ for the second clock state and we indicate that the minimum RMSE corresponds to τ ranging from 10 s to 100 s. We notice that the error reduction in the last decade of τ in Fig. 3 is caused by the finite database.

THE THIRD CLOCK STATE (LINEAR FRACTIONAL FREQUENCY DRIFT RATE)

In a like manner, measurements are provided for the third clock state termed the linear fractional frequency drift rate. The results are shown in Fig. 4. Here, a minimum RMSE fits the region of τ from 300 s to 600 s. For this minimum, the optimal N is provided by Fig. 4 exactly, even though, on the whole, the $N_{0(opt)}$ was found with some error. We notice again that the last decade in the τ scale (from 10^3 s to 10^4 s in Fig. 4) is not reliable to make conclusions for, owing to the finite database.

THE FOURTH CLOCK STATE (QUADRATIC FRACTIONAL FREQUENCY DRIFT RATE)

To evaluate N_{opt} and τ_{opt} for the fourth clock state that may be called the quadratic fractional frequency drift rate, the only algorithm may be used, that is (15)–(18). Accordingly, Fig. 5 gives one curve for $N_{0(opt)}$ and the other one for the RMSE vs. τ. The principal observation is that the minimum RMSE lies likely in the last decade of τ from 10^3 to 10^4 or even beyond this decade. This is not unexpected, since the frequency changes very slowly even in crystal oscillators. Therefore, the spectral content associated with the quadratic drift rate inherently places very closely to zero and much time is necessary to evaluate the $N_{0(opt)}$ and $\tau_{0(opt)}$. Nevertheless, one may conclude that, even approximately, the quadratic fractional frequency drift rate may be estimated by the unbiased FIR algorithm with τ_{opt} about 3 hours with only a couple of points in the average.

MEASUREMENTS AND ESTIMATIONS OF THE TIE

Provided τ_{opt} and N_{opt} for every clock state (Figs. 3–6), we compare the unbiased FIR estimates to the sawtooth corrected GPS-based measurements.

ALMOST LINEAR TREND OF THE TIE

In the first experiment, we selected the part of the process in which the TIE of a crystal clock undergoes almost linear regular changes. Following Fig. 3, the time step was set to be τ = 1 s and we set N = 2060 and N = 2050 to estimate the TIE from the measurements with and without the sawtooth correction, respectively, in the minimum MSE sense. The results are shown in Fig. 7. The first point to notice is that the RMSE of the measurements obtained with the sawtooth correction is 4.67 ns that coincides with the facilities of the correction. The linear FIR estimates (6) applied to measurements without and with the sawtooth correction were found to be, respectively, 1.6 ns and 1.69 ns, which is substantially lower than in the sawtooth-corrected measurements. An additional observation shows that noise in the estimates is also lowered, having no excursions, contrary to measurements. Certainly, for the near linear trend, the unbiased FIR estimates look superior to the sawtooth correction.

ALMOST QUADRATIC TREND OF THE TIE

For the second experiment, we found a region where the TIE changes almost quadratically (Fig. 8). The optimum numbers were found here to be N = 920 and N = 790 for measurements with and without the sawtooth correction, respectively. We notice that these values are consistent to those shown in Fig. 3 at τ = 1 s. The RMSE error of the sawtooth-corrected measurements was calculated to be 7.5 ns. Almost the same errors, 8.0 ns, and 7.5 ns, were found in the estimates obtained from measurements without and with the sawtooth correction, respectively. Because the nonlinear case is more regular, we conclude that the sawtooth correction and the estimation produce almost the same RMSEs. However, like in Fig. 7, the noise in the estimates is still substantially lower and excursions are almost fully smoothed.

COMPLEX FUNCTION OF THE TIE

We finally examined measurements with a somewhat sophisticated behavior of the TIE (Fig. 9). The optimum numbers were found to be N = 1150 and N = 1120 (with and without the correction, respectively). F or these values, the RMSEs of the estimates were calculated to be 7.83 ns, and 8.0 ns, respectively, and the RMSE of the sawtooth-corrected measurements was evaluated by 8.87 ns. Again, we watch for the comparable results and notice that noise and excursions are still much more suppressed in the estimates.

MEASUREMENTS AND ESTIMATIONS OF THE FRACTIONAL FREQUENCY OFFSET

By the algorithm (Fig. 1), measurements and estimates of the second clock state $x_2(n) = y(n)$ (fractional frequency offset) are provided with the discrete-time derivatives applied to the TIE. Accordingly, measurements of the fractional frequency offset are formed by $[\hat{x}_1(n) - \hat{x}_1(n-1)]/\tau$, where $\hat{x}_1(n)$ should be treated to be either the TIE measurements with the sawtooth correction or the estimates of the TIE obtained by the unbiased FIR filter. By the results given in Fig. 4b, the minimum error of the $x_2(n) = y(n)$ estimate is obtained with $\tau = 10 \ldots 100$ s. We therefore set $\tau = 100$ s, since it corresponds to a lower optimum number N (Fig. 4a), thus a smaller computational time. The results of measurements and estimations are shown in Fig. 10. Only 20 points were enough to provide a minimum RMSE in the estimates. We therefore set N = 20 to a simple averaging (5) and filter the time derivatives of both estimates of the TIE, namely with and without the sawtooth correction.

Fig. 10a demonstrates that the derivative of the reference measurement fits, on the whole, the derivative of the GPS-measurement with the sawtooth correction. It is also seen that the GPS-measurement produces much larger noise, which standard deviation reaches 55.6×10^{-12}. The latter value may be treated as a resolution in frequency of the GPS-based sawtooth-less measurements. Contrarily, the unbiased FIR estimates (Fig. 10b) produce much lower noise and trace very close to Rb-measurements. Indeed, the standard deviations of the differences between the reference curve and two estimates (without and with the sawtooth correction) were evaluated at the levels of, respectively, 15.0×10^{-12} and 13.4×10^{-12}. Fig. 10c demonstrates how well the estimates fit the Rb-measurements. For the comparative purposes, in Fig. 10d, we show the estimates obtained by the linear FIR function. For this filter, the RMSEs have appeared to be larger, respectively, 16.7×10^{-12} and 14.6×10^{-12}. The latter means that the algorithm is correct suggesting the uniform kernel (5) for the second clock state.

CONCLUDING REMARKS

In this paper, we presented the results of the experimental comparison of the GPS-based TIE measurements (with and without the sawtooth correction) and unbiased FIR estimation for a local crystal clock. We also brought the relevant plots to evaluate the optimal time step τ_{opt} and optimum number of the points N_{opt} in the average for the uniform, linear, quadratic, and cubic kernels employed by the unbiased FIR filtering algorithm (Fig. 1). The conclusions are as follows.

The optimal values τ_{opt} and N_{opt} differ for different clock states. For the crystal clock imbedded in the Stanford Frequency Counter SR620, the first state (TIE) must be filtered with $\tau = 1$ s and the relevant N_{opt} taken from Fig. 3a. The second state (fractional frequency offset) is estimated with $\tau = 10 \ldots 100$ s and the relevant N_{opt} provided by Fig. 4a. The third state (linear fractional frequency drift rate) needs setting τ

= 300 … 600 s with N_{opt} taken from Fig. 5a. Finally, the fourth state (quadratic fractional frequency drift rate) may be evaluated with τ of more than 10^4 s and only several points in the average.

An experimental comparison of the GPS-based measurements with the sawtooth correction and the relevant unbiased FIR estimates of the TIE model of a local crystal clock led to the following conclusions:

• GPS-based sawtooth-less measurements represent basically the mean value of its origin (without correction) with a small amount of noise. Therefore, the unbiased filter applied to either of these measurements produce almost the same output (Figs. 7b, 8b, 9b, and 10b).

• The real-time unbiased FIR filtering algorithm (Fig. 1) efficiently suppresses noise and smoothes excursions featured to sawtooth-less measurements.

• The unbiased FIR filter produces much lower errors for the fractional frequency offset and higher degree states owing to the lower noise intensity in the estimates of the TIE.

Overall, owing to small noise and smoothed excursions in the estimates, the unbiased FIR filtering algorithm (Fig. 1) may be considered to be more efficient than the sawtooth-less measurements, whenever accurate evaluation of the TIE model of a local clock is needed.

REFERENCES

[1] T. A. Clark and R. M. Hambly, 2006, *"Improving the Performance of Low-Cost GPS Timing Receivers,"* presented at this Meeting but not submitted for publication in these Proceedings.

[2] R. M. Hambly and T. A. Clark, 2003, *"Critical Evaluation of the Motorola M12+ GPS Timing Receiver vs. the Master Clock at the United States Naval Observatory, Washington, DC,"* in Proceedings of the 34th Annual Precise Time and Time Interval (PTTI) Systems and Applications Meeting, 3-5 December 2002, Reston, Virginia, USA (U.S. Naval Observatory, Washington, D.C), pp. 109-115.

[3] Y. S. Shmaliy, 2002, "*A Simple Optimally Unbiased MA Filter for Ttimekeeping,"* **IEEE Transactions on Ultrasonics, Ferroelectrics, and Frequency Control, UFFC-49,** 789-797.

[4] Y. S. Shmaliy, 2006, *"An Unbiased FIR Filter for TIE Model of a Local Clock in Applications to GPS-based Timekeeping,"* **IEEE Transactions on Ultrasonics, Ferroelectrics, and Frequency Control, UFFC-53,** 862-870.

[5] L. Arceo-Miquel, Y. S. Shmaliy, J. Munoz-Diaz, and O. Ibarra-Manzano, 2006, *"Experimental Comparison of the Unbiased FIR Estimation vs. the Sawtooth Correction in GPS-Based Timekeeping,"* in Proceedings of the 2006 IEEE International Frequency Control Symposium, 5-7 June 2006, Miami, Florida, USA (IEEE), pp. 604-608.

[6] J. Munoz-Diaz, Y. S. Shmaliy, L. Arceo-Miquel, and O. Ibarra-Manzano, 2006, *"Investigation of an Optimum Sampling Interval for a Local Clock TIE Model with an Uunbiased FIR Filtering Algorithm,"* in Proceedings of the 2006 IEEE International Frequency Control Symposium, 5-7 June 2006, Miami, Florida, USA (IEEE), pp. 589-603.

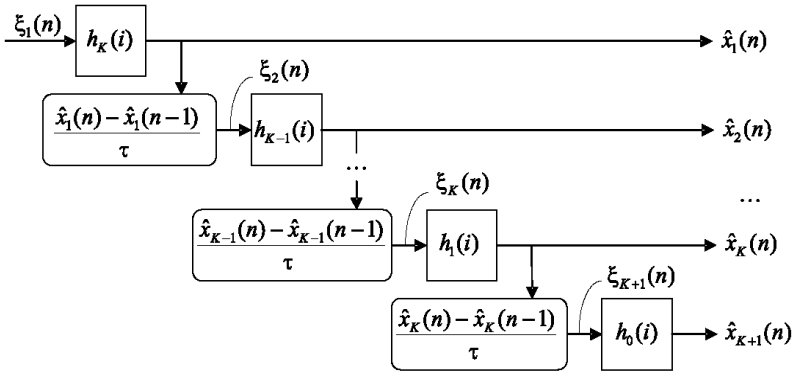

Figure 1: Structure of the unbiased FIR filtering algorithm for the TIE model of a local clock.

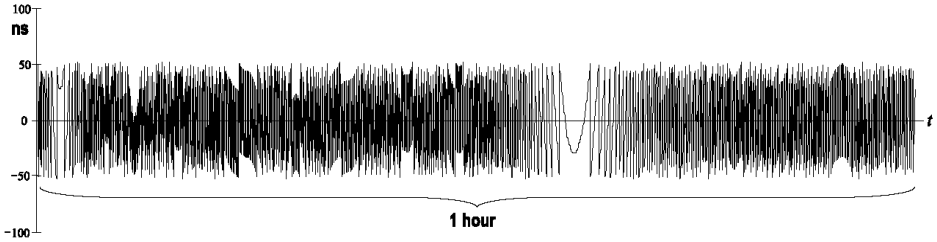

Figure 2: Typical structure of the sawtooth noise induced by the GPS timing sensor SynPaQ III.

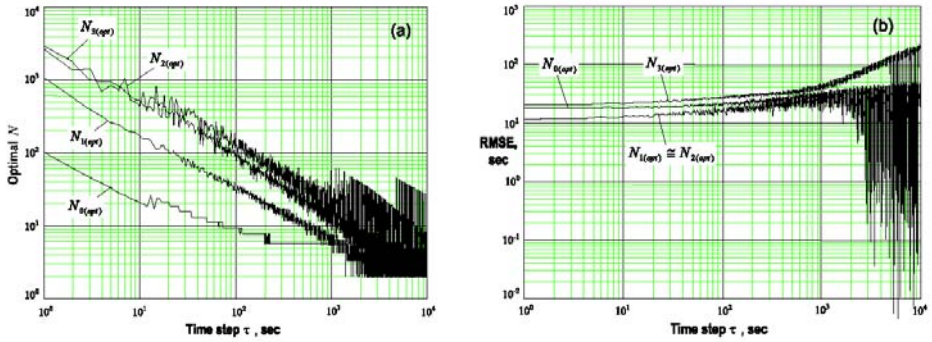

Figure 3: Optimal N_{opt} vs. τ for the first clock state (TIE): (a) optimal N and (b) RMSE.

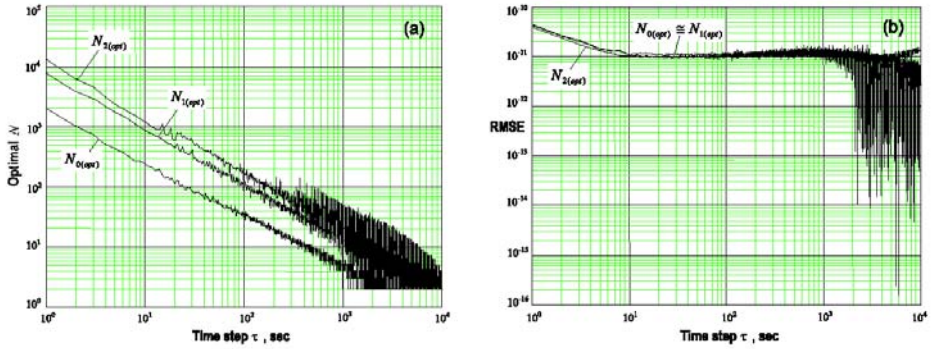

Figure 4: Optimal N_{opt} vs. τ for the fractional frequency offset: (a) optimal N and (b) RMSE.

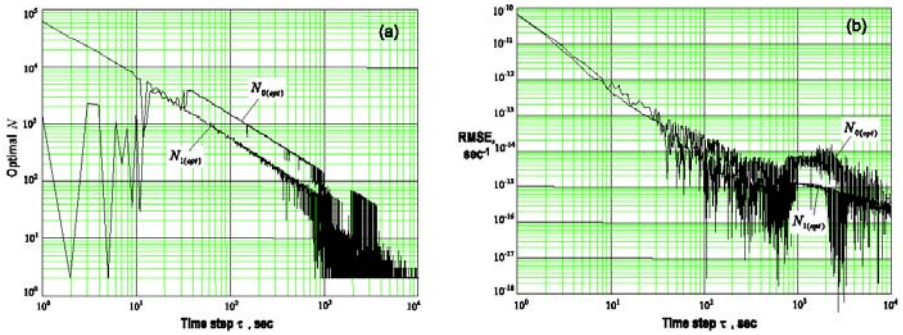

Figure 5: Optimal N_{opt} vs. τ for the linear fractional frequency drift rate: (a) optimal N and (b) RMSE.

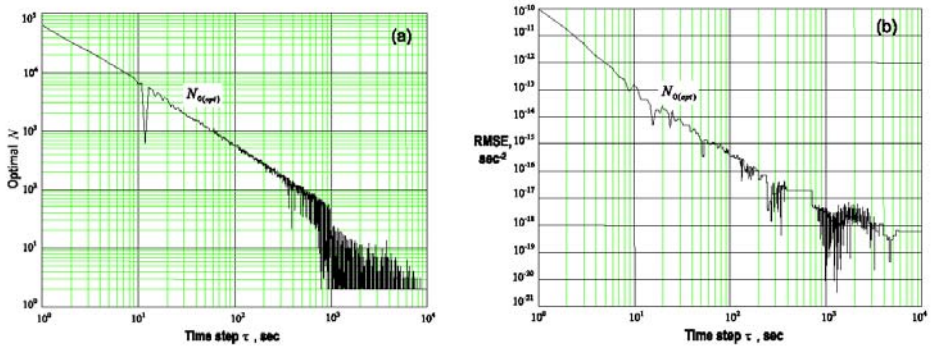

Figure 6: Optimal N_{opt} vs. τ for the quadratic fractional frequency drift rate: (a) optimal N and (b) RMSE.

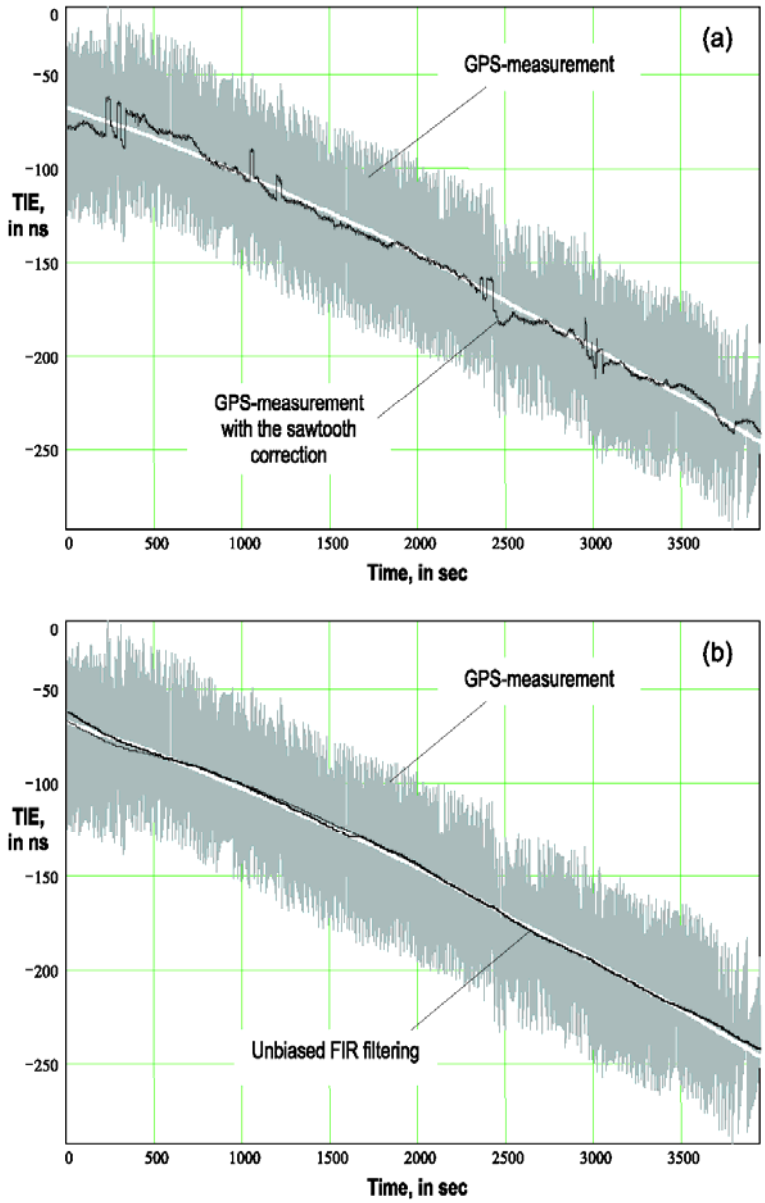

Figure 7: Unbiased FIR filtering vs. the sawtooth correction: (a) GPS-based measurements with and without the sawtooth correction and (b) filtering of the TIE with (light) and without (bold) the sawtooth correction using the linear unbiased FIR filter. White curve is by the reference Rb-measurements.

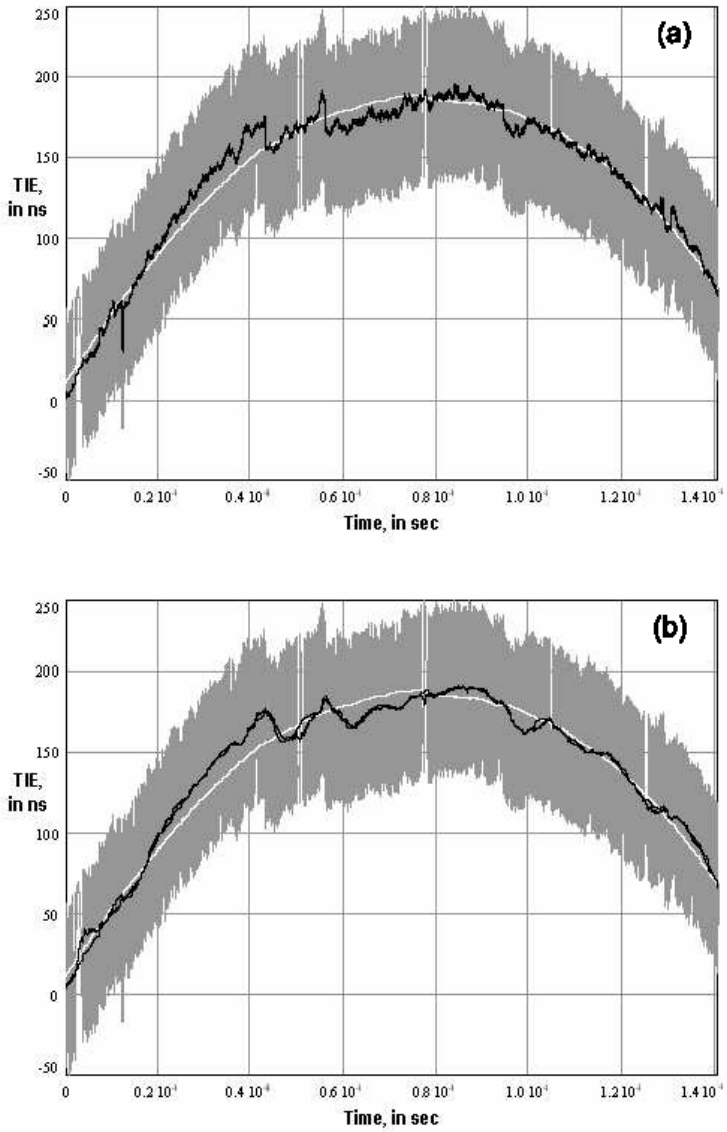

Figure 8: Unbiased FIR filtering vs. the sawtooth correction: (a) GPS-based measurements with and without the sawtooth correction and (b) filtering of the TIE with (light) and without (bold) the sawtooth correction using the linear unbiased FIR filter. White curve is by the reference Rb-measurements.

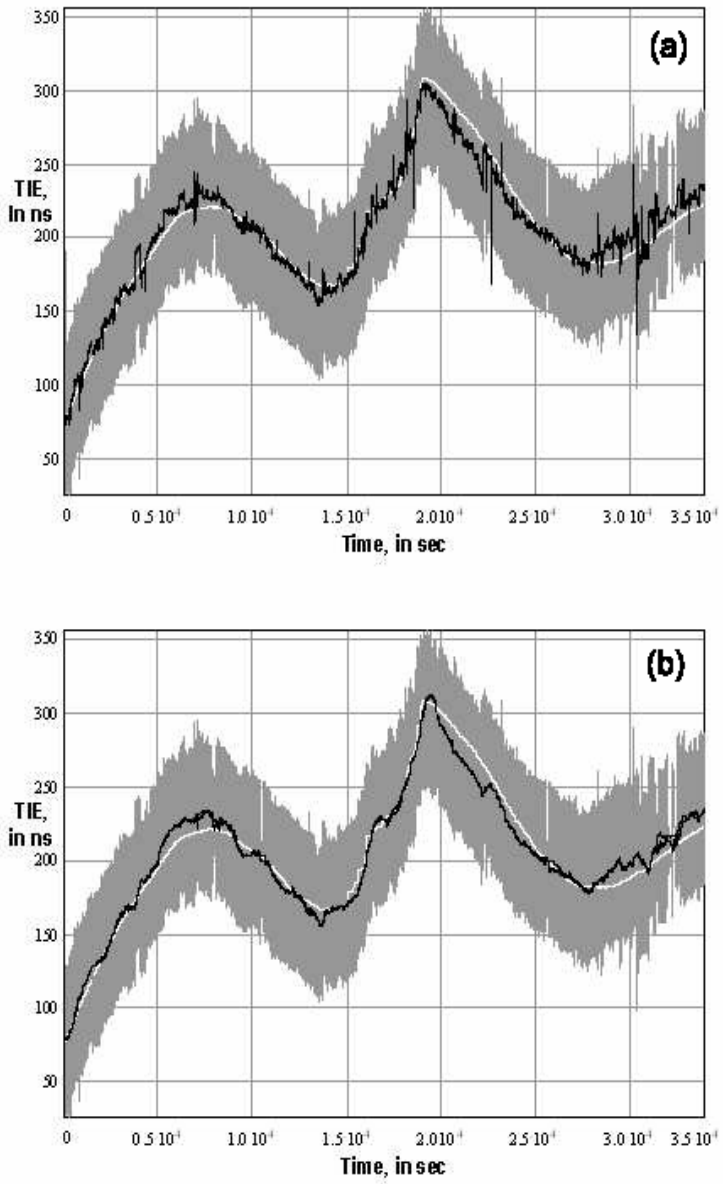

Figure 9: Unbiased FIR filtering vs. the sawtooth correction: (a) GPS-based measurements with and without the sawtooth correction and (b) filtering of the TIE with (light) and without (bold) the sawtooth correction using the linear unbiased FIR filter. White curve is by the reference Rb-measurements.

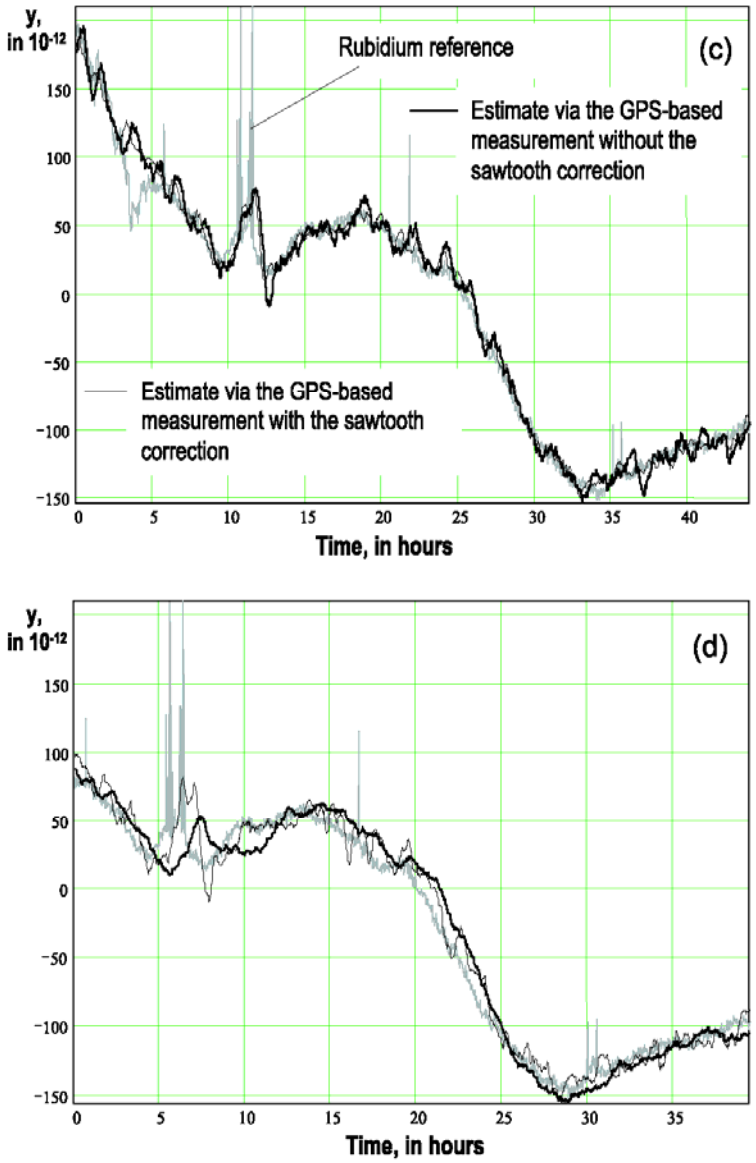

Figure 10: Unbiased FIR filtering of the second clock state vs. the sawtooth correction: (a) GPS-measurements with the sawtooth correction and Rb-measurements, (b) unbiased FIR filtering of the measurements with (light) and without (bold) the sawtooth correction, (c) unbiased FIR filtering with a uniform kernel (5) vs. the Rb-measurements, and (d) unbiased FIR filtering with a linear kernel (6) vs. the Rb-measurements (the curve labels are the same as in (c)).